LITERATURE REVIEW

Nanostructured Material

Nanoscale materials are considered to be the building blocks for nanotechnology and are referred to particles having at least one dimension less than 100 nm (Biswas and Wu, 2005). Nanoparticle posses large surface areas and essentially no inner mass, that is, their surface-to-mass ratio is extremely high. They are of the immense scientific interest in recent years. They can be used in various nanoscopic structure areas. They are also important in polymer, powder and biotechnology industries such as magnetic, electronic, biomedical, pharmaceutical, cosmetic, energy, catalytic, and materials applications, as well as in environmental protection (Pratsinis, 1998; Biswas and Wu, 2005; Kojima and Baba, 2005; Theodore and Kunz, 2005).

1. Applications of Single Component and Composite Nanoparticles

Pure oxide nanoparticles are already being produced on a variety of industrial scales. The sizes of nanoparticles make it possible to design and produce new materials with improvement of their physical properties. Silicon dioxide (SiO_2) is one of the major products that have a lot of usage for industry (Pratsinis, 1998; Jang, 1999; Pol *et al.*, 2004; Akurati *et al.*, 2006). It is used as additives in plastics and rubbers to improve mechanical properties of elastomers and to improve the suspension behavior (Jang, 1999; Pol *et al.*, 2004) and antibacterial activity in liquid systems (Adams *et al.*, 2006). Aluminum oxide (Al_2O_3) can exist in a large variety of crystallographic forms. For instance, γ-, δ- and θ-Al_2O_3, called transition aluminas, are metastable forms of Al_2O_3 and are widely employed as adsorbents, supports for catalysts, coatings and soft abrasives, while α-Al_2O_3 is the most stable Al_2O_3 polymorph and is usually crystallized at high temperatures (Macedo *et al.*, 2007). They can be used as ceramic materials because of their heat and abrasion resistance properties and inert behavior in corrosive media (Lindackers *et al.*, 1998). For TiO_2 nanoparticles, they are well known that pure TiO_2 has many useful applications depending on its crystal phase, for example, rutile has been used in the pigment industry while anatase is known for photocatalytic activity (Pratsinis, 1998). Moreover, it can be used in cosmetic for high absorption of ultraviolet radiation (Jang, 1999) and for toxic metal capture (Wu *et al.*, 1998; Lee and Hyun, 2006).

SiO_2-based nanocomposite has more potential for improvement of performance when compared to the single-component nanoparticle (Akurati *et al.*, 2006). SiO_2/TiO_2 nanostructure has been extensively used in paint pigments, optical-chemical sensors, glasses, supporting materials and catalysts (Lee *et al.*, 2007). The combination of SiO_2 with Al_2O_3 has been widely used for insulators, electronic, steel coating, catalytic properties and adsorption of heavy metals (Elliott and Huang, 1981; Huang and Rhoads, 1989; Wei *et al.*, 2001; Kuo and Chuang, 2002). Their applications depend upon the crystal phase and morphology of the particles. The different morphologies are also utilized in different applications. For example, core shell structures of TiO_2-coated SiO_2 is used as catalyst and SiO_2-coated TiO_2 is used for paint opacifiers (Vemury and Pratsinis, 1995). The TiO_2 cores are covered with varying precipitation and adsorption layers to modify the pigment to suit better the system and the working environment because pure TiO_2 reflects efficiently all visible light. The dispersion of Al_2O_3 and/or SiO_2-coated TiO_2 pigment samples in acrylic-isocyanate automotive paints were reported (Johansson *et al.*, 1993). The pure silica coating to TiO_2 consumed less dispersion and wetting agent than with a mixed coating.

Consequently, to control morphology and crystal phase of the particles is imperative step toward designing advanced material for different applications.

2. Nanozeolites with Microporous Materials

Several excellent review articles were dedicated to different aspects of zeolite applications, synthesis and recent development appeared in the past 3 years (Tosheva and Valtchev, 2005). Two important properties of microporous materials are ion exchange and gas sorption (Bu and Feng, 2003). The ion exchange is the exchange of ions held in the cavity of microporous materials with ions in the external solutions.

The gas sorption is the ability of a microporous material to reversibly take in molecules into its void volume.

Tosheva and Valtchev (2005) focused on the synthesis, crystallization mechanism and application of colloidal zeolites and nanosized zeolites were considered having size of less than 1,000 nm (Tosheva and Valtchev, 2005). Microporous materials are porous solids with pore size below 20 Å. Porous solids with pore size between 20 and 500 Å are called mesoporous materials. Macroporous materials are solids with pore size larger than 500 Å. The development of crystalline microporous materials started in late 1940s with the synthetic of zeolites (Bu and Feng, 2003). Crystalline microporous materials generally have a narrow pore size distribution. This makes it possible for a microporous material to selectively allow some molecules to enter its pores and reject other molecules that are either too larger or have a shape that does not match with the shape of the pore. A number of applications involving microporous materials utilize such size and shape selectivity.

Zeolites

1. Definition of Zeolites

A strict definition of zeolites is difficult because both chemical compositions and geometric features are involved. Zeolites can be loosely considered as crystalline three-dimensional aluminosilicates arising from a framework of $[SiO_4]^{4-}$ and $[AlO_4]^{5-}$ (Dyer, 1988) with open channels or cages. Frameworks of zeolites are based on four-connected network of AlO_4 and SiO_4 tetrahedral linked together through the corner-sharing of oxygen anions. In a zeolite framework, oxygen atoms are bi-coordinates between two tetrahedral cations. When describing a zeolite framework, oxygen atoms are often omitted and only the connectivity among tetrahedral atoms is taken into consideration.

A framework type is determined based on the connectivity of tetrahedral atoms and is independent of chemical compositions, types of extra-framework species, crystal symmetry, unit cell dimensions, or any other chemical and physical properties. This is because the term 'structure' implies both the framework and the extra-framework constituents of a zeolite and the latter are excluded in the framework description. Even taking into consideration of both zeolites and non-zeolites, synthetic and natural solids, 176 framework type codes (consisting of three capital letters) have been assigned to date (Baerlocher and McCusker, 2007) listed in the 6th edition of the “Atlas of Zeolite Framework Types” published by the structure commission of the International Zeolite Association (2007).

In the absence of the framework interruption, the overall framework formula of a zeolite is AO_2 just like SiO_2. When A is Si^{4+}, no framework charge is produced. However, for each Al^{3+}, a negative charge develops on the framework. The negative charge is balanced by either inorganic or organic cations located in channels or cages of the framework. The charge-balancing cations are usually mobile and can undergo ion exchange.

Not all zeolites are microporous because some are unable to retain their framework once extra-framework species (e.g., water or organic molecules) are removed. The stability of zeolites and catalytic properties vary greatly depending on framework topologies and chemical compositions such as the Si/Al ratio, the type of charge-balancing cations and location of metal clusters and their interaction with the framework (Bhatia, 1990; Bu and Feng, 2003).

Bu and Feng (2003) reported that synthetic zeolites fall into two families on the basis of extra-framework species. One family is similar to natural zeolites in chemical compositions. These zeolites have a low Si/Al ratio that is usually less than 5. The other family of zeolites are made with organic structure-directing agents and they generally have a Si/Al ratio larger than 5.

An empirical rule, Loewenstien rule (Loewenstein, 1954), suggests that in zeolites, only Si-O-Si and Si-O-Al linkages be allowed. In other words, the Al-O-Al linkage does not occur in zeolites and the Si/Al molar ratio is ≥ 1.

2. Type of Zeolites

An important structural parameter is the size of the pore opening through which molecules diffuse into channels and cages of a zeolite. The pore size is related to the ring size defined as the number of tetrahedral atoms forming the pore (Bu and Feng, 2003). In the literature, zeolites with 8-rings, 10-ring, and 12-ring windows are often called small-pore, medium-pore, and large-pore zeolites, respectively. The pore volume of a zeolite is related to the framework density defined as the number of tetrahedral atoms per 1000 $Å^3$. In general, the framework density does not reflect the size of the pore openings. For zeolites, the observed values range from 12.7 for faujasite to 20.6 for cesium aluminosilicate (CAS) (Baerlocher *et al.*, 2001). Even for the same framework topology, a change in the chemical composition will lead to a change in bond distances and consequently in unit cell volumes. This will result in either an increase or decrease in the framework density.

All zeolites are built from TO_4 tetrahedra, called primary (or basic) building units. Large finite units with three to sixteen tetrahedral (called Secondary Building Units or SBU's) are often used to describe the zeolite framework (Baerlocher *et al.*, 2001). The smallest SBU is a 3-ring, but it rarely occurs in zeolite framework types. Instead, 4-rings and 6-rings are most common in zeolite and zeolite-like structures. The simplest classification describes all known zeolite framework as arrangement linking eight 8 SBU's ; single four ring (S4R), single six ring (S6R), single eight ring (S8R), double four ring (D4R), double six ring (D6R), complex 4-1, complex 5-1 and complex 4-4-1 (Dyer, 1988).

In the past three decades, efforts directly related to synthetic aluminosilicate zeolites are generally in the area of high silica (Si/Al > 5) or pure silica molecular sieves (Bu and Feng, 2003). The use of organic bases has had a significant impact on the development of high silica zeolites. The Si/Al ratio in the framework is increased because of the low charge to volume ratios of organic molecules. In general, the crystallization temperature (100-200°C) is higher than that required for the synthesis of hydrated zeolites. Alkali-metal ions, in addition to the organic materials, are usually used to control the pH and promote the crystallization of high silica zeolites.

Low ($Si/Al \leq 2$) and intermediate ($2 < Si/Al \leq 5$) silica zeolites are used as ion exchangers and have also found use as adsorbents for applications such as air separation. Syntheses of low and intermediate zeolites are usually performed under hydrothermal conditions using reactive alkali-metal aluminosilicate gels at low temperatures (~100 °C and autogeneous pressures). The synthesis procedure involves combining alkali hydroxide, reactive forms of alumina and silica, and H_2O to form a gel. Crystallization of the gel to the zeolite phase occurs at a temperature near 100 °C.

3. Zeolite Synthesis from Sol-Gel Method

Sol-gel processing is a wet-chemical method that allows high-purity, high-homogeneity nanoscale materials to be synthesized at lower temperatures compared to competing high-temperature methods (Theodore and Kunz, 2005). A significant advantage that sol-gel science affords over more conventional materials-processing routes is the mild conditions that the approach employs.

Two main routes and chemical classes of precursors have been used for sol-gel processing (Theodore and Kunz, 2005).

1. Colloidal route (inorganic route), which uses metal salts in aqueous solution (chloride, oxychloride, nitrate) as raw materials. These are generally less cost and easier to handle than the metal-organic route. However, their reactions are more difficult to control and the surfactant that is required by that process might interfere later in downstream manufacturing and end use.

2. Alkoxide route (metal-organic route) in organic solvents. This route typically employs metal alkoxides M(OR)Z as the starting materials, where M is Si, Ti, Zr, Al, Sn, or Ce; OR is an alkoxy group; and Z is the valence or the oxidation state of the metal. Metal alkoxides are preferred because of their commercial

availability and the high lability of the M-OR bond. They are available for nearly all elements and cost-effective methods. A larger range of mixed-metal nanoparticles can be produced under mild conditions, often at room temperature, by mixing metal alkoxides (or oxoalkoxies) and other oxide precursors.

In general, the sol-gel process consists of the following steps: sol formation, gelling, shape forming, drying and densification. First, after mixing the reactants, the organic or inorganic precursors undergo two chemical reactions: hydrolysis and condensation or polymerization, typically with an acid or base as a catalyst, to form small solid particles or clusters in a liquid (either an organic or aqueous solvent).

The resulting solid particles or clusters are so small (1 to 1,000 nm) that gravitational forces are negligible and interactions are dominated by van der Waals, coulombic, and steric forces. These sols, colloidal suspensions of oxide particles, are stabilized by an electric double layer, or steric repulsion, or a combination of both. The colloidal particles then link together by further condensation and a dimensional network occurs. As gelling proceeds, the viscosity of the solution increases dramatically.

The chemistry of the sol-gel process (Klein, 1991) can be simplified to:

Hydrolysis: $\mathrm{M(OR)_x + H_2O \rightarrow M(OR)_{x-1}OH + ROH}$

Condensation-Polymerization: $\mathrm{2M(OR)_{x-1}OH \rightarrow (OR)_{x-1}M\text{-}O\text{-}M(OR)_{x-1} + H_2O}$

The sol-gel can be formed into three different shapes: thin film, fiber, and bulk. Thin (100 nm or so) uniform and crack-free films can readily be formed on various materials by lowering, dipping, spinning, or spray coating techniques.

Sol-gel chemistry is promising, yet it is still in its infancy and a better understanding of the basic inorganic polymerization chemistry has to be reached.

Some drawbacks include the high cost for the majority of alkoxide precursors, relatively long processing times, and high sensitivity to atmospheric conditions. Moreover, the batch nature of present sol-gel processing leaves cost and scale-up issues associated with the development of viable continuous production routes.

Zeolites are normally crystallized from aqueous alkaline gels containing sources of silica, alumina and cations (Catlow, 1992). Crystallization may take hours or weeks and is usually undertaken in the temperature range of ~60-200 °C and under autogeneous pressure. The nature of the product is controlled by kinetic factors and small changes in the conditions can alter the products (Bhatia, 1990; Catlow, 1992) For example, variation of the inorganic base can result in a different range of products.

Okada and Mackenzie (2006) reported that many zeolites were synthesized using quaternary ammonium hydroxides (R_4NOH, R: CH_3-, C_2H_5-, C_3H_7-, C_4H_9-, etc) as organic templates. The relationships between the templates and the synthesized zeolites are shown schematically in Figure 1. The organic templates dissolve in alkaline solutions as R_4N^+ ions, forming large tetrahedral structures. Aluminosilicate anions electrostatically surround the R_4N^+ ions and form crystalline three-dimensional framework structures under hydrothermal conditions. Zeolites are thus obtained after removal of the organic template by calcination at several hundred degrees censius. Although the organic templates R_4NOH form relatively large hydrated cations in solution, the resulting sizes are limited to the micropore range (< 1 nm). By contrast, long chain alkyl ammonium ions having hydrophobic and hydrophilic groups in the head and tail are known to form micelles within certain concentration and temperature ranges.

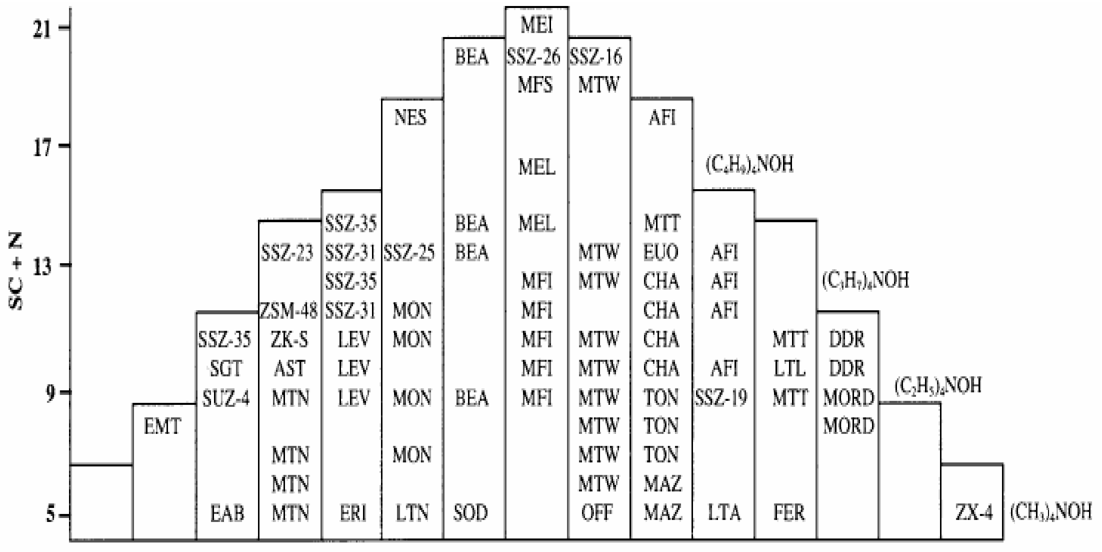

Figure 1 Relationship between structure-directing agents (SDA) and the resulting zeolites.

Source: Okada and Mackenzie (2006)

The area of zeolite membrane has been the subject of intense researches during the last decade (Caro *et al.*, 2000). Zeolite membranes are inorganic aluminosilicate crystalline films grown on porous supports (Gardner *et al.*, 2002). Au and Yeung (2001) reported that zeolite with its well-defined, nanometer sized pore structure is an attractive material for inorganic membrane separation. Small (i.e. 0.3-0.4 nm with 6- and 8-membered ring), medium (i.e. 0.5-0.6 nm with 10-membered ring) and large pore (i.e. 0.7-0.8 nm with 12-membered ring) zeolites have been successfully made into membranes (Au and Yeung, 2001). This is due to their prominent characteristics, which are unique to zeolite materials: pore openings used for molecular sieving, metal-ion exchanging and are common to inorganic membrane: thermal resistance and organic solvents resistance. For this reason, they can be used at high temperature and with organic solvents, when polymeric membranes cannot operate (Algieri *et al.*, 2001). Mostly, research on zeolite membranes frequently focuses on ZSM-5. These zeolite membranes on porous ceramic and metal supports were prepared with various thicknesses (5-100 μm) by in situ crystallization (Vroon *et al.*, 1996). There are various types of zeolite membrane preparation.

1. Using the synthetic zeolite from coating of a porous supporter with a colloidal solution by dip-coating or spin-coating (Wong *et al.*, 2001a; Wong *et al.*, 2001b).

2. Using the in-situ crystallized zeolite (ZSM-5 mainly) coated on mesoporous supporter, i.e., alumina, metal, silica that can be categorized into two types:

2.1 Hydrothermal synthesis with/without seeds: In terms of synthesis with seeds crystal supported crystallization, there are both of the same and different zeolites (Dong *et al.*, 1998; Xomeritakis *et al.*, 1999; Algieri *et al.*, 2001; Au *et al.*, 2001; Bernal *et al.*, 2001; Bonilla *et al.*, 2001; Sterte *et al.*, 2001; Wan *et al.*, 2001; Takata *et al.*, 2002). For direct in-situ crystallization without seeds (Masuda *et al.*, 2001; Romanos *et al.*, 2001), use of electrophoretic technique from negatively-charged zeolite particles could actually attract the zeolite particles to the substrate surface before they precipitate out of the solution (Oonkhanond and Mullins, 2001).

2.2 Dry gel conversion method: CVD technique used for precursor gel drying to crystallize on supporter, called dry synthesis (Kikuchi *et al.*, 1997; Nishiyama *et al.*, 1997).

4. Applications of Zeolites and Zeolites Membrane

Zeolites are routinely used in three main areas of industrial chemistry. The largest is heterogeneous catalyst. Older but important applications are in ion exchange and gas separation (Catlow, 1992). The regular nanoporous networks of zeolites and other crystalline molecular sieves have been put to extensive and increasing use for separations (Mohanty and McCormick, 1999).

In 1992, Catlow summarized that it is important to understand the relation between the structure of a zeolite and the adsorption of specific molecules. However, the theory of adsorption and transport in zeolites is incomplete. The zeolitic framework allows the adsorbed molecules to move, in a potential of varying magnitude and sign. In order to get a rough measure of the volume accessible to the adsorbed molecules one can consider the boundary surfaces on which the potential is zero; but this approach is very limited. The molecules are localized by the repulsive part of this potential field, and the extent of this localization depends on the temperature and other thermodynamic variables.

In 2003, Bu and Feng reported that traditional zeolites are microporous inorganic solids with aluminosilicate tetrahedral building units, which possess accessible internal cavities that capable of binding guest molecules and catalyzing chemical reactions. Zeolites are used for the production of many consumer products ranging from gasoline to detergents and contribute to almost a trillion dollars of global economy annually. For example, size selective heterogeneous catalytic transformation of petrochemicals has been extensively used to improve the quality of gasoline, and thus significantly reduce the pollution of incomplete combustion of fossil fuels.

There are many studies have shown catalytic activity for lean-NO_x reduction with a variety of using unburned hydrocarbons such as ethylene, propylene, propane, decane, and so on. They pointed out that large-and medium-pore zeolite structures with MFI (ZSM-5), MOR, FAU, FER and IM5 exchanged with different cations (e.g. Cu, Pt, Ag, Fe, Co, Ce, Rh, Pd, Ni, Mn and Ga) have been studied (Subbiah *et al.*, 2003). With a few different approaches for lean-NO_x reduction, the selective catalytic reduction of NO_x by using hydrocarbons (Hydrocarbon-Selective Catalytic Reduction; HC-SCR) as reductants has been attracting the most attention. However, all zeolite-based catalysts, Cu/ZSM-5 in particular, have major problems due to both of hydrothermal degradation from permanent deactivation and negative sensitivity towards water vapor.

The best results, the maximum conversion of 64% at 350 °C, have generally been achieved with ZSM-5 (MFI) zeolite structure when exchanged with Cu. On the other hand, Cu/ZSM-5 has major problems on hydrothermal degradation resulted in decrease of NO_x conversion by 24% at 800°C and hydrothermal de-alumination of the zeolite framework has also been a major issue in the permanent deactivation of the catalyst, especially Cu/ZSM-5 (Grinsted *et al.*, 1993; Yan *et al.*, 1995; Subbiah *et al.*, 2003).

The NO_x reduction of diesel or lean-burn gasoline engines exhaust achieved by certain catalysts. This task is easier for stationary engines, as in power plants, where the options for the reductant are wider than for automotive vehicles. The most efficient reductant is ammonia, which is better result than hydrocarbon, zeolite-based catalyst Fe/ZSM-5 in particular (Chen *et al.*, 2004). Novel techniques were developed to prepare zeolite-based catalysts. For instance, the chemical vapor deposition (CVD) technique was used to sublime $FeCl_3$ into the acid form of a zeolite, such as ZSM-5. This led to catalysts with much higher Fe loading than can be achieved by conventional ion exchange from an aqueous solution (Chen and Sachtler, 1998).

Zeolites exhibit physical adsorption properties in which hydrocarbons are trapped within the zeolite pores (Namba *et al.*, 1984). They also exhibit chemical adsorption capabilities at point of unbalanced electric charges resulting from the addition of Al, which can bond the hydrocarbons.

In part of zeolite membrane application, industrial applications of inorganic membranes, particularly ceramic membranes, for separation activities like ultrafiltration, nanofiltration, wastewater treatment and gas separation are now well established and the preparation and characteristic of ceramic membrane substrate or support play an important role in asymmetric ceramic membrane that deposited on it (Li and Zhong, 2002). Porous ceramics are used as gas/liquid separators, catalyst supports and molecular sieves which can be used at high temperature and severe chemical conditions (Chen *et al.*, 2005a).

There are several authors reported gas separation through ZSM-5 (MFI-type) zeolite membranes to separate CO_2/CH_4 (Poshusta *et al.*, 1999), n-C_4H_{10}/i-C_4H_{10} (Aoki *et al.*, 2000), CO/air (Piera *et al.*, 2002), H_2/N_2, H_2/CH_4, H_2/C_4H_{10}, He/N_2, He/SF_6, He/Ar (Au and Yeung, 2001) and *p*-xylene/*o*-xylene (Sakai *et al.*, 2001). There are some using ZSM-5 membranes in catalytic membrane reactor (CMR) for the oxidehydrogenation of propane (ODP) (Bottino *et al.*, 2002), methylation of toluene (Takata *et al.*, 2002) and reaction of methanol to olefins (Masuda *et al.*, 2003).

SUZ-4 Zeolite

SUZ-4 is a new synthetic zeolite and was first synthesized and patented by the British Petroleum Company (Barri, 1992). The proposed SUZ-4 framework consists of five-, six-, eight-, and ten-membered rings and with the ten-membered rings having pore openings minimum of 4.6 Å and maximum of 5.2 Å (Lawton *et al.*, 1993) while Figure 2a shows minimum of 4.1 Å. The SUZ-4 topology consists of a three dimensional pore system having straight ten-membered ring channels intersected by two arrays of eight-membered ring channels at an angle of about 74° and they are in the plane [001], perpendicular to the direction of the ten-membered-ring channels and small cages linked through double six-membered ring as shown in Figure 2 (Lawton *et al.*, 1993; Lukyanov *et al.*, 1999). The crystal system type is orthorhombic and its growth is to be small needle shaped particle (Gujar and Price, 2002).

In 2006, framework of SUZ-4 zeolite which is one of seven new framework type codes was recently accepted by the International Zeolite Conference with the structure code namely SZR ($|K^+_4|$ $[Al_4Si_{32}O_{72}]$-SZR) orthorhombic, Cmmm (No. 65) with a = 18.8064, b = 14.2298 and c = 7.4548 Å, $\alpha = 90.0$, $\beta = 90.0$ and $\gamma = 90.0$ and framework density: 18 T/1000Å^3.

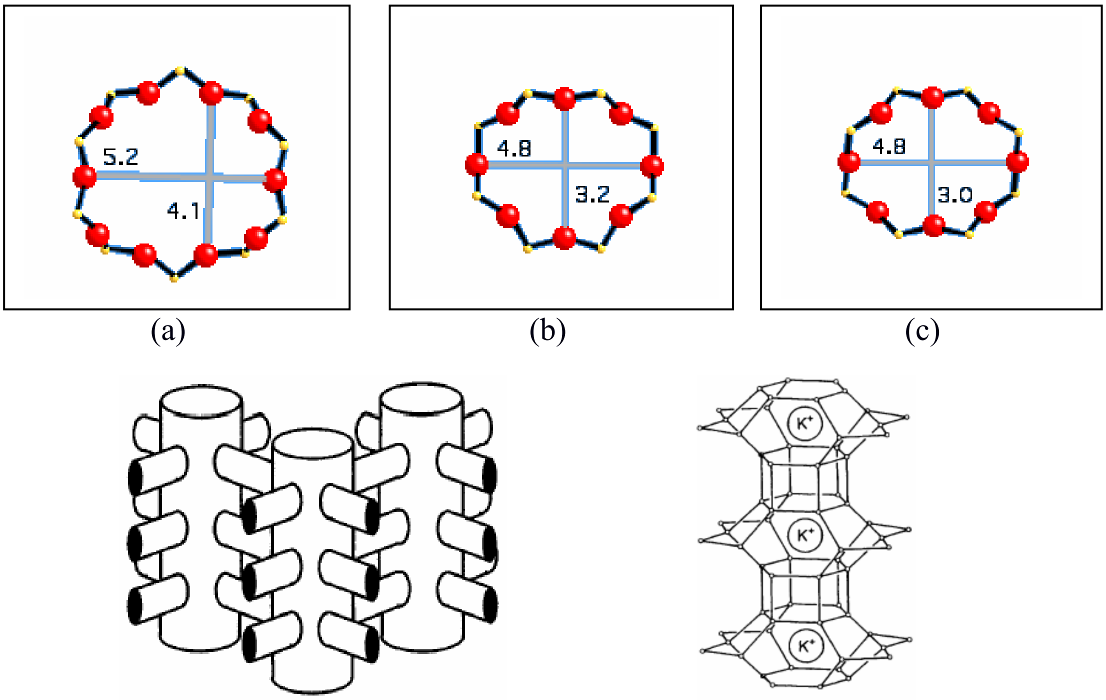

(a) (b) (c)

(d) (e)

Figure 2 SUZ-4 zeolite topology and scheme (a) 10-ring viewed along [001] 4.1 x 5.2 Å (b) 8- ring viewed along [010] 3.2 x 4.8 Å and (c) 8-ring viewed along [110] 3.0 x 4.8 Å (3-dimensional) (d) schematic representation of SUZ-4 multichannel system (e) columns along the unit cell c-axis

Source: Baerlocher and McCusker (2007); Lawton *et al.* (1993); Lukyanov *et al.* (1999); Strohmaier *et al.* (2006)

In addition, FTIR characterization of acid sites in SUZ-4 in comparison with ferrierite was reported that destruction of the spectrum, supported by H-D exchange and accessibility studies, results in three IR bands at 3560, 3592, and 3610 cm^{-1} corresponding to OH groups in 6-, 8- and 10-membered rings (Zholobenko *et al.*, 1998). Moreover, forms of SUZ-4 zeolite in the low frequency region of the Raman spectra to the various T-O-T vibrations and to the cation-oxygen vibration modes containing transition metal ion exchanged zeolites (e.g. Cu, Mn and Fe) have been studied using Raman spectroscopy (Gujar *et al.*, 2005).

Mostly synthetic step of SUZ-4 zeolite has used structure directing agents (SDA), which is tetraethylammonium hydroxide (($(C_2H_5)_4NOH$, TEAOH) (Asensi *et al.*, 1999; Price, 2001; Okada and MacKenzie, 2006). A newer template, *N*,*N*,*N*,*N*′,*N*′,*N*′-hexaethylpentanediammonium bromide (Et_6-diquat-5) has been emerged (Paik *et al.*, 2000) and reported to give SUZ-4 with higher Si/Al ratios than TEAOH. The ^{1}H-^{13C} CP MAS NMR, Raman spectra of Et_6-diquat-5 ions encapsulated SUZ-4 zeolite and molecular modeling studies were presented and conformation of guest molecule and the geometry of the host structure are observed for the medium-pore SUZ-4 zeolite, revealing the existence of organic structure-directing effect (Paik *et al.*, 2001).

Furthermore, structure directing agents having a series of flexible diquaternary alkylammonium ions $(C_2H_5)_3N^+(CH_2)_nN^+(C_2H_5)_3$ (Et_6-diquat-n with n = 3-10) for SUZ-4 zeolite synthesis in the present of alkali metal cation were studied. Among the organic structure agents, a considerable diversity in the phase selectivity, especially to the type and concentration of alkali cations used, was observed only for the Et_6-diquat-5 can produce SUZ-4 zeolite (Lee *et al.*, 2003).

Kim et al. (2004) reported that the reproducible synthesis of SUZ-4 zeolite crystals was synthesized with TEAOH as a template under vigorous stirring condition. Crystal morphology of SUZ-4 was finely tuned by various H_2O/SiO_2 ratios. Reaction parameters such as pH, concentration of precursor sol and reaction time also influenced the morphology and crystallinity of zeolite crystals. Good crystalline of SUZ-4 was obtained above 250 rpm. Calcined samples were characterized by BET, NH_3-TPD, XRD, and SEM.

The new type of zeolite namely SUZ-4 zeolite has been claimed to be a very effective de-NO_x catalyst as well as a very useful catalyst for many hydrocarbon reactions (Asensi *et al.*, 1999). In 2003, Subbiah *et al.* attempted to find the better hydrothermal stability of Cu/SUZ-4 and K/SUZ-4 compared with Na/ZSM-5. Each zeolite sample was treated at 800 °C for 4 h under a flowing gas mixture of 5% oxygen and 2.5% water vapor in nitrogen. Primarily, the observation of no loss of tetrahedral peak intensity of the aged Cu/SUZ-4 confirmed that there was no de-alumination in the Cu/SUZ-4 structure. Even though, the K/SUZ-4 (the un-exchanged zeolite) lost about 29% of its tetrahedral Al on aging. The Na/ZSM-5 structure was found to have the most extensive de-alumination losing 65% of its tetrahedral aluminum from the framework as estimated from Al MAS NMR experiments. It shows that SUZ-4, which is high hydrothermal stability, is appropriate in reducing lean-NO_x.

In addition, new catalytic property of SUZ-4 on very selective formation and stable catalyst for producing dimethyl ether in methanol dehydration were also found because the formed dimethyl ether is hardly converted to hydrocarbons (Jiang *et al.*, 2004), different from ZSM-5 zeolite that methanol can be further produced to olefins. Choo *et al.* (2001) studied in palladium-exchanged SUZ-4 zeolite (PdHK-SUZ-4) catalytic activity of ethylene dimerization using electro spin resonance (ESR) spectroscopy and the results showed that the adsorbate reduceed Pd(II) to Pd(I) at 20 °C, leading to the formation of two Pd(I) ions situated at two different sites of SUZ-4. One was the same Pd(I) ion site formed by thermal reduction but it appeared at higher intensity upon adsorption. The other Pd(I) was an isolated Pd(I) produced only after prolonged annealing with adsorbates. They also described that within the small cages where one site was probably more difficult to reduce than the other and the observation of Pd(I) mostly remaining after adsorption of CO on SUZ-4 further supported that the Pd(I) produced after thermal reduction was located in the small cages (Choo *et al.*, 2001).

Furthermore, the catalytic properties of the proton form of 10-ring zeolite of SUZ-4 zeolite were compared with clinoptilolite, ferrierite, ZSM-22, ZSM-57 and ZSM-5 zeolites for the skeletal isomerization of 1-butene to isobutene and it was found that pore shape of 10-ring channels of medium-pore zeolite was found to be the key parameter substantially governing the isomerization activity (Lee *et al.*, 2004a). The results revealed that the more elliptical 10-ring channels the zeolite had, the lower 1-butene conversion but the higher initial isobutene selectivity it showed. However, chemical analysis indicated that H-SUZ-4 for their study still contains a considerable amount (2.7 wt %) of K^+ ions even after NH_4^+ ion exchange and the effect besided from ellipticities of their 10-ring channels that were the effects of other factors including the zeolite crystal size and morphology could also be of considerable importance.

In addition, the skeletal isomerization of a hydrocarbon feedstock process for converting n-butenes to the corresponding isobutene was patented by the BP Chemicals Ltd. (Atkins and Smith, 1994).

Nanoparticles from Flame Aerosol Synthesis

1. Flame Aerosol Reactors

There are several synthesis methods currently available to produce nanoparticles. Liquid and gas phases are two common techniques for nanomaterials production (Koch, 2002). Among the gas phase methods, flame aerosol reactor (FLAR) is one of the widely used technologies for the formation of nanosized particles. It can produce high purity material in single step with short production time and is scaled-up easily to industrial level (Ehrman *et al.*, 1998; Lindackers *et al.*, 1998; Pratsinis, 1998). FLAR allows nanosized particles to be built from molecules as desired. Starting from clusters of molecules nanoparticles are then formed by coagulation and sintering in the hot flame environment (Stark *et al.*, 2001). It also creates crystals of complex chemical structures those are useful in producing multicomponent material at relative low cost compared to other routes. In addition, FLAR enables continuous production, while liquid method is often performed in a batch system (Akurati *et al.*, 2006).

The flame conditions, e.g., flame temperature, gas flow rate and residence time, and precursor concentration ratio are the main parameters that determined mixed oxide growth processes (Hung and Katz, 1992; Bakrania *et al.*, 2007). The morphology of the mixed oxide particles is the result of interactions between two or more oxides. These interactions include the nucleation of the primary particles, particle-particle collisions, growth of one oxide onto the other, melting, and formation of composite phase. In order to obtain different morphologies and crystal phases, we need to understand the effects of corresponding parameters in binary phase system for nanocomposite material. It is possible that differences in the chemical reaction kinetics of the precursors affect the species arrangement for multicomponent aerosols.

2. Formation of Single and Mixed Oxides particles

Formations of single species oxide, e.g., TiO_2, SiO_2 and Al_2O_3, by the flame method are reported in many articles. In the case of nanosized TiO_2, the growth, particles aggregation, and agglomerate structure as a function of flame height are the major topics studied (Yang and Biswas, 1997). The roles of synthesis methods on nanostructured TiO_2 were thoroughly reviewed (Pratsinis, 1998) and the particle size was also found to affect on the apparent photoactivity of TiO_2 in water (Skandan *et al.*, 1999). There are some studies on Al_2O_3 powder synthesis. It was synthesized by oxidation metalorganic precursors in premixed $H_2/O_2/Ar$ low pressure flames (Lindackers *et al.*, 1998) and acetylene/O_2/Air for the combustion flame-chemical vapor condensation (Skandan *et al.*, 1999). The results showed their size depended on the precursor concentration and the sampling position (Lindackers *et al.*, 1998). Besides, fume silica was also synthesized by many researchers (Jang, 1999; Wooldridge *et al.*, 1999; Pol *et al.*, 2004).

Vemury and Pratsinis (1995) studied the effect of dopants on the characteristics of TiO_2 particles and concluded that the addition of $SiCl_4$ decreased the sintering rate of TiO_2 and primary particle size. In contrast, a decrease in crystal size of TiO_2 came from an increase in the iron dopant concentration (Wang *et al.*, 2001). Size of segregated phase of mixed-oxide can be controlled by changing the O_2 flow rate for binary TiO_2/SiO_2 and SnO_2/SiO_2 nanoparticles system (Akurati *et al.*, 2006). Synthesis of SiO_2/TiO_2 at different flame heights from the surface of the burner in a H_2/O_2 co-flow diffusion was shown that the chemical composition of Si decreases with increasing height from burner furnace and increased mobility of the aggregates (Suh *et al.*, 2006). The formation of TiO_2-SiO_2 particles from $TiCl_4$ and $SiCl_4$

precursors in a H_2/O_2 counter flow diffusion flame burner was investigated and found that morphology strong depended on temperature (Hung and Katz, 1992).

Mercury Emission Control with Nanostructured Materials

Nanostructured materials are of major importance in the environment, both as potential pollutants and as pollution control substances (Biswas and Wu, 2005). Research has shown that many physical and chemical properties depend on particle size in the nanometer-size range (Almquist and Biswas, 2002; Li *et al.*, 2006).

In environmental applications, nanomaterials are turning out to be remarkably effective tools for cleaning up contaminated sources. One application is using them as sorbents for capture of heavy metals from contaminated aqueous waste streams (Bailey *et al.*, 1999; Masciangioli and Zhang, 2003; Diallo and Savage, 2005; Savage and Diallo, 2006) and from combustion sources (Owens and Biswas, 1996; Biswas and Wu, 1998). Several materials have been studied for heavy metal capture from gas phase exhausts (Biswas and Wu, 1998; Jurng *et al.*, 2002). For example, agglomerated nanostructured silica sorbents have been shown to be very effective at capturing cadmium species compounds in high temperature environments from a combustion system (Lee *et al.*, 2005).

There are several kinds of sorbent used for heavy metal removal (Bailey *et al.*, 1999; Jurng *et al.*, 2002). Alumina was proved to be more effective for capture of Be and Ni than silica under typical conditions in coal combustion and solid waste incineration (Biswas and Wu, 1998). Alumino-silicate pillared montmorillonite (MMT) and an in-situ generated agglomerated silica have been proposed for the capture of cadmium species (Lee *et al.*, 2005). Low-cost sorbents have been studied for the removal of heavy metals from solution, such as zeolites, clinoptilolite, and fly ash (Bailey *et al.*, 1999). Moreover, the use of natural zeolites as soil additives was able to reduce mercury in plants (Haidouti, 1997).

1. Elemental mercury

Mercury is a persistent toxin that can result in serious damage to the respiratory, nervous, and gastrointestinal systems. It is one of the trace metals (As, Be, Cd, Co, Cr, Hg, Ni, Mn, Pb, Sb and Se) that the Environmental Protection Agency (EPA) has included for potential control under the Clean Air Act Amendments (US EPA, 2005). Mercury exists in three forms: elemental mercury, inorganic mercury compounds (primarily mercuric oxide and chloride), and organic mercury (primarily methyl mercury) (Lee, 1999). In the atmosphere, elemental mercury is by far the most common form and, as a vapor, it is responsible for the long-range, global cycling of mercury (Brigden *et al.*, 2002). Although the primary mercury exposure route to humans is through the consumption of fish, the major source of anthropogenic mercury emissions in the U.S. is from coal burning utilities. Public concern over mercury emissions led to EPA issuing the Clean Air Mercury Rule (CAMR) on March 15, 2005, which aims to reduce total mercury emissions from coal burning utilities in the U.S. through a market-based cap and trade system (US EPA, 2005).

For coal-fired power plants in Thailand, toxic and potentially toxic elements in fly ash were studied by Greenpeace Research Laboratories, UK (Brigden *et al.*, 2002). Mae Moh power plant with a total capacity greater than 2,500 megawatt (MW) produces 4,380,000 tons of fly ash along with 39 tons of the neurotoxin mercury annually. The results of the heavy metal and metalloid analyzes of the fly ash samples are presented in Table 1. Fly ash sample contained arsenic and mercury at concentrations above concentrations typically found in uncontaminated soils by three and fourteen times respectively. The presence of elemental mercury of these concentrations is of concern, as it is extremely toxic and is usually found in very low levels in the environment. Moreover, the potential environmental hazards from the ash as a result of very large quantity of ash produced, and some toxic chemicals can be leached from the ash into the immediate environment.

Table 1 Concentrations of elements identified in samples of fly ash from similar coal fired power facilities.

Fly ash producer	Mae Moh, MI02011, Thailand	4 coal power plants, Greece	1050MW coal power plants, Spain	11 coal power plants, UK	Coal fly ash, China
Element	Concentration (mg/kg dry weight)				
Arsenic (As)	172	NA	60	40-205	NA
Cadmium (Cd)	<1	11.6-14.4	1.3	0.13-0.82	312-315
Calcium (Ca)	108604	NA	39700	NA	NA
Chromium (Cr)	39	110-160	134.2	NA	NA
Cobalt (Co)	16	NA	29.2	NA	NA
Copper (Cu)	52	31.8-62.8	71.8	NA	NA
Lead (Pb)	22	123-143	52.0	17-176	843-847
Manganese (Mn)	566	213-330	324.6	NA	NA
Mercury (Hg)	8.8	NA	0.01	NA	8.1-8.3
Nickel (Ni)	36	NA	87.9	NA	NA
Zinc (Zn)	156	59.6-86.9	221.3	NA	NA

Source: Brigden *et al.* (2002)

Current control technologies are not very effective at reducing emissions of elemental mercury compared to the removal of other pollutants such as fine particles and sulfur dioxide. While several mercury control technologies are being developed, they have not yet been commercially deployed. Activated carbon is one of the most widely tested sorbents and has displayed the capability of removing elemental and oxidized mercury from flue gas streams. However, its application in real combustion environments is limited due to its high cost, requirement of high carbon-to-mercury ratio, and problems with disposal of the resultant fly-ash (Lee *et al.*, 2006). Alternate approaches of mercury capture in coal combustion processes such as with inorganic sorbent addition have been shown to be effective in reducing both gaseous and particle-bound mercury in the exhaust. Coal combustion processes with sorbent addition has been shown to effectively capture gaseous mercury and suppress the fraction in the solid phase (Biswas and Wu, 1998; Granite *et al.*, 2000; Sjostrom *et al.*, 2002).

Potential sorbents for injection include activated carbon and inorganic based sorbents (e.g. TiO_2). Many control technologies are significantly less effective at reducing emissions of elemental mercury compared to other forms. Installation of an SCR catalyst specifically for the purpose of mercury oxidation does not appear to be an economical choice (Presto and Granite, 2006). Optimized technologies for mercury control are being developed and demonstrated but they are not yet commercially deployed. The solid phase speciation of mercury in combustion byproducts dictates its leachability to the environment and it can be investigated using sequential extraction techniques (Wang *et al.*, 2004). Sequential extractions furnish information of the future mobility of mercury in the environment and indicate the ability of a sorbent to sequester mercury (Tessier *et al.*, 1979). The mobility of heavy metals depends on the strength of bond between the heavy metal and the solid matrix and the composition of the leaching solution (Filgueiras *et al.*, 2002). The goal of a sequential extraction is to differentiate among metals bound to different solid phases and mineral fractions (Ariza *et al.*, 2000).

2. Differential Bed Reactors

While the feasibility of such sorbents in capture of heavy metals species has been demonstrated, there is a need for further study to ensure wider applicability. One important aspect is the rate of capture of the heavy metals. The availability of kinetic data can then be used to select the appropriate sorbent, design and guide operational conditions for the capture processes (Biswas and Wu, 1998; Bailey *et al.*, 1999).

Differential bed reactor (DBR) systems are commonly used to evaluate the effectiveness of sorbents by performing gas-solid kinetics studies (Mahuli *et al.*, 1997; Agnihotri *et al.*, 1998; Jadhav and Fan, 2001; Lee *et al.*, 2004b). Two important steps that control rate of gas-solid reaction are the external mass transfer and the surface reactions. The differential bed reactor enables the minimization of the external mass-transfer resistance; therefore, the overall rate of metal adsorption can be determined solely from the surface interaction.

Mercury capture efficiency is dependent on a combination of physical (morphology and size) and chemical (crystalline phase) properties (De Lasa *et al.*, 2005). In addition, Noel et al. (2007) described an approach to study the binding characteristics of mercury to sorbent material. While there are many studies examining the feasibility of sorbents for mercury capture (Wu *et al.*, 1998; Jurng *et al.*, 2002; Lee *et al.*, 2006; Li and Wu, 2007), there is still a need to develop a methodology for sorbent selection based on the rates of reactions.

Photocatalytic Oxidation

Photocatalytic processes have been newly receiving much attention, particular for the destruction completion or mineralization of the toxic and non-biodegradable compounds to carbon dioxide and inorganic constituents. Photocatalyst is defined as a substance that is activated by the absorption of a photon and helps accelerate a reaction without being consumed. The factors that influence the photocatalyst activity include structure, particle size, surface properties, preparation, spectral activation, and resistance to mechanical stresses (De Lasa *et al.*, 2005). The strong oxidative potential of the positive holes oxidizes water to create hydroxyl radicals under UV light irradiation. It can also oxidize oxygen or organic materials directly. Among the photocatalysts applied of heterogeneous photocatalysis, TiO_2 is considered as one of the most promising material to decompose indoor volatile organic compounds (Zhang and Liu, 2004).

Dye wastewater is one of the industrial wastes, which is difficult to degrade and it is environmentally serious. It is feasible to use TiO_2 as a catalyst to degrade many kinds of dye compounds, but it is found out that methyl orange dye was more difficult to degrade than other dye compounds (Keiichi *et al.*, 2000). Binary mixed oxides were developed to improve the separated efficiency from particles agglomeration of TiO_2 in wastewater system. The photocatalytic properties of the SiO_2-TiO_2 pillars were investigated in the degradation of methyl orange in water using nanometer-sized SiO_2-TiO_2 sols aggregates in acidic solution and ion exchange reaction into clay from natural Na-montmorillonite (Liu *et al.*, 2006) and Ag loaded on $TiO_2/\gamma\text{-}Al_2O_3$ leaded to efficient photodecolorization of methyl orange (Chen *et al.*, 2005b). Silica-embedded nanocrystalline TiO_2 powders were synthesized by sol-hydrothermal process and the photocatalytic activity of samples for decomposition of 1,4-dichlorobenzene was revealed that addition of SiO_2 to TiO_2 brought an increase in the photocatalytic activity (Kim *et al.*, 2006). In addition, silica-loaded TiO_2 has been reported to enhance the photocatalytic degradation of tetramethylammonium in water (Vohra *et al.*, 2005), degrading ethylene (Fu *et al.*, 1996), rhodamine 6G (Anderson and Bard, 1997) and cyanide (Ahmed and Attia, 1995). In similar context, the as-prepared TiO_2/SiO_2 composite nanoparticles from hydrothermal and sol-gel synthesis showed more improved photocatalytic activity than pure anatase-type TiO_2 from the decomposition of methylene blue (Hirano and Ota, 2004). SiO_2-TiO_2 mesoporosous materials with TiO_2 dispersed uniformly on silica supports have been prepared by a novel method of hydrolysis and condensation could prevent agglomeration and also increased photodegradation of methyl orange (Zhang *et al.*, 2005). The floating $TiO_2{\cdot}SiO_2$ photocatalyst beads were prepared by the dip-coating method and the amount of SiO_2 influences the photocatalytic activity of $TiO_2{\cdot}SiO_2$ beads (Shifu and Gengyu, 2005).

In addition, to prevent photocatalytic properties of TiO_2 particles with organic compounds, TiO_2 surface should be covered with a stable oxide layer. SiO_2 coated TiO_2 nanoparticles were synthesized by a sol-gel process and demonstrated that photocatalytic activity and UV shielding effect were suppressed from amorphous SiO_2 layer testing by photodegradation of Rhodamine B (Park *et al.*, 2004).